A Microwave Compatible MIC Temperature Electrode for Use in Biological Dielectrics

LAWRENCE E. LARSEN, ROBERT A. MOORE, SENIOR MEMBER, IEEE, JOHN H. JACOBI, MEMBER, IEEE, F. A. HALGAS, AND P. V. BROWN

Abstract—**A microwave compatible four-terminal electrode design based on hybrid microwave integrated circuit (MIC) construction is presented. The concept of electrothermal matching is employed to prevent artifact in either of two directions: heat sourcing and heat sinking. The electrode system includes a temperature-encoding electronic package. The electrode is designed for use in the brain at a specific insertion depth. It has been tested by thermographic methods for electromagnetic properties at 2450 MHz and a power density of ~250 mW/cm². The system has been thermometrically evaluated for calibration stability and freedom from hysteresis. Stability and artifact has been shown to be within ±0.15°C independent of temperature cycling and/or thermal history.**

I. Introduction

THIS COMMUNICATION reports the further development of a temperature measurement system for *in situ* use in tissues other than bone during microwave exposure. The first report described a transducer system based on hybrid microwave integrated circuit (MIC) construction [1]. This transducer was designed to operate in a biological dielectric exposed to incident fields up to 50 mW/cm^2 with field disturbance equivalent to a thermal aberration less than 0.1°C [2]. The first paper concluded with an allusion to problems due to the temperature coefficient of and excessive heating in the transmission line interposed between the transducer and the resistance measurement instrumentation. The line used at that time was carbon-loaded polytetraflouroethylene (PTFE) developed at the National Bureau of Standards [3].

Subsequently, a microcircuit resistance bridge and bypass *RC* networks were added to the upper substrate section. This design removed the PTFE line connecting the resistance measurement section to the transducer subassembly. Unfortunately, field coupling to the transducer subassembly was increased. This design was not developed further. The combined heating of four PTFE lines seriously limited use of this configuration.

A second approach to the problem of resistance measurement was pursued by Cetas [4]. After testing the integrated bridge electrode in fields of 150-mW/cm^2 incident power density, Cetas correctly concluded that the electrode was not adequately decoupled for use in diathermy fields of this intensity. He modified the electrode by removal of the microcircuit bridge, but the design did retain the four transmission lines and transducer subassembly in a four-terminal design for resistance measurement [5]. Cetas also increased the lineal resistance of the microline in the transducer subassembly, in order to increase its decoupling for use in higher power density fields. This version of the MIC electrode was considered usable in tissues other than bone, at power densities 2–3 times higher than the original design goals.

The further development of this electrode is the subject of the present communication. The four-terminal design was retained, but the four-terminal point was moved from the top of the upper substrate section to the sensor in order to remove any effects due to the temperature coefficient of the interposed microline. In addition, the sensor was changed to a glass-encapsulated thermistor from the thick-film thermistor used previously to provide a stable microenvironment for the thermistor. The thermistor resistance/temperature (RT) curve is a function of the ratio of oxidized to reduced states in the semiconductor slurry after firing. This proportion of states is effected by the microenvironment of the thermistor. Long-term RT stability requires the equilibration of oxidation and reduction and the maintenance of a stable microenvironment by glass encapsulation.

Gold microline in the quadplanar thin-film conductor configuration was tested, then abandoned. Field transmission was increased in this configuration possibly due to slot mode propagation [6]. In addition, the photolithographic fabrication required by this method was not amenable to volume production or easy change in length. As a result, the thin-film gold microline was replaced with a gold–ruthenium–paladium (GRP) thick-film conductor. The thick-film conductors were distributed on four arcs, evenly spaced, around a hollow cylindrical substrate.

The PTFE line continued to be a problematic component in the system. The lineal resistance of the line was steadily increased in order to reduce heating. This line operated in air, and required ever higher resistance to operate in this low-loss environment. However, lineal resistances less than or equal to 100–150 kΩ/in made it difficult to fabricate reliable connections to the line. Over

Manuscript received August 9, 1978; revised March 5, 1979. Portions of this work were presented at the 1976 USNC International Union of Radio Science Annual Meeting, Amherst, MA.

The authors are with Walter Reed Army Institute of Research, Department of Microwave Research, Washington, DC, and Westinghouse Electric Corp., Baltimore, MD. The views of the authors do not purport to reflect the positions of the Department of the Army or the Department of Defense. (Para. 4-3, AR 360-5.)

time, the junction impedance increased and the electrode became sensitive to mechanical artifact. In addition, the PTFE line demonstrated unequivocal standing waves when placed parallel to the direction of polarization of the electric field. These factors lead to the development of a new line which will be subsequently described.

Lastly, experiments with the transducer subassembly *sans* transmission line demonstrated that heat sinking would be a problem if the line was to become adequately decoupled. These findings prompted the development of the concept of electrothermal matching whereby the electrode could contribute artifact, either through heat sourcing or heat sinking, when compared to the losses in the displaced volume of tissue. These factors lead to the development of an improved transducer subassembly with spatially varying impedance for operation in tissue, for operation at the tissue/air interface, and a short segment for operation in air where the new transmission line was attached.

II. Methods

The fabrication methods include a combination of thick- and thin-film techniques. Thick-film techniques were used for the four-terminal transducer subassembly. Thin-film techniques were used for the transmission line.

The thick-film construction began with cylindrical, hollow porcelain substrate approximately 2 in long, 20-mil outer radius, and 3–5-mil wall thickness. The GRP paste finally used had a specific resistance of 50-Ω per square. The paste was applied over a screen with linearly tapering cross section, in order to taper the lineal resistance from approximately 200 kΩ/in at the proximal portion of the transducer subassembly to a value of approximately 50 kΩ/in at the distal end (the values were measured in approximately half-inch segments from each end of the line). The gold portion of the paste provided the "low" resistance component, the ruthenium provided attachment to the substrate, and powdered silicon provided passivation when the composite was fired. The result is a glass-passivated line which is virtually immune to scratching, and degradation in physiological or hydrocarbon media.

The glass-encapsulated thermistor was attached after shorting the four lines into two pairs at the distal end with minute amounts of conductive epoxy. In this way the thin-film lines could be attached and the lineal resistance verified without the presence of a temperature sensitive resistance. The sensor was supplied (VECO 52A19) with two short stubs of 2-mil wire (PtIr) which were removed. The result was two "pads" that were flush with the glass. These pads were used for connection to the shorted pairs of thick-film line, the last step in the fabrication.

The thin-film line was fabricated by vacuum deposition of nichrome on 2-mil thick polished mylar substrate. The vacuum deposition took place through a mask with a constant 10-mil width. Resistance was monitored during the nichrome deposition as a means to reduce variability. The deposition was controlled to result in a line of 200-kΩ/in lineal resistance. The line was fabricated in 6-in strips. The conductor thickness was approximately 30 Å. The ends were then processed through a second deposition for a 1-mil thick pad of aluminum over the terminal 0.200 in of the nichrome. The final deposition was for a uniform SiO_2 passivation.

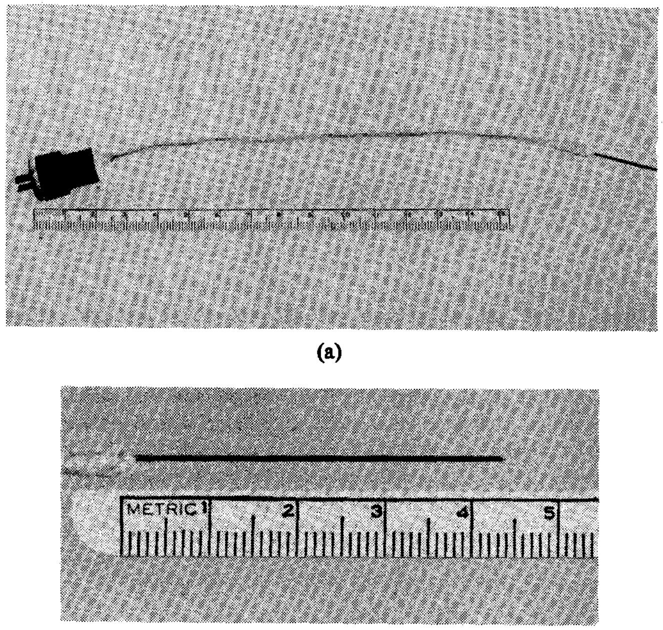

Fig. 1. (a) A panoramic view of the completed hybrid MIC electrode. The tubing contains four hyperthin lines on Mylar substrate. (b) A closer view of the transducer subassembly which shows the four-terminal point at the sensor.

The four finished lines were attached to the proximal end of the transducer subassembly by minute amounts of conductive epoxy. All junctions were strain relieved with clear nonconductive epoxy. A fabrication problem due to the use of thermal setting epoxy was discovered. The electrode was thermal cycled 12–14 times up to about 100°C in the fabrication process. These thermal cycles caused minute fractures in the thin film at the region near the aluminum pad. Presumably, these fractures were due to different coefficients of expansion for the thick aluminum and the thin nichrome. The result was that production yields were extremely low (about 15 percent) and the finished electrodes open circuited after durations from a few days to two weeks. Presently, only room temperature setting epoxies are used. The completed electrode is shown in Fig. 1(a) and (b).

The four thin-film lines were covered in Tygon tubing of 40-mil ID and 60-mil OD. The proximal ends of the four thin-film lines were then attached to a 4-pin connector with an intermediate piece of substrate and point-to-point 1-mil gold wire. The entire interior of the connector shell and tubing were potted and strain relieved with nonconductive epoxy.

Power densities were always 247 mW/cm^2 incident, and duration was either 15 or 30 s. Short exposures are

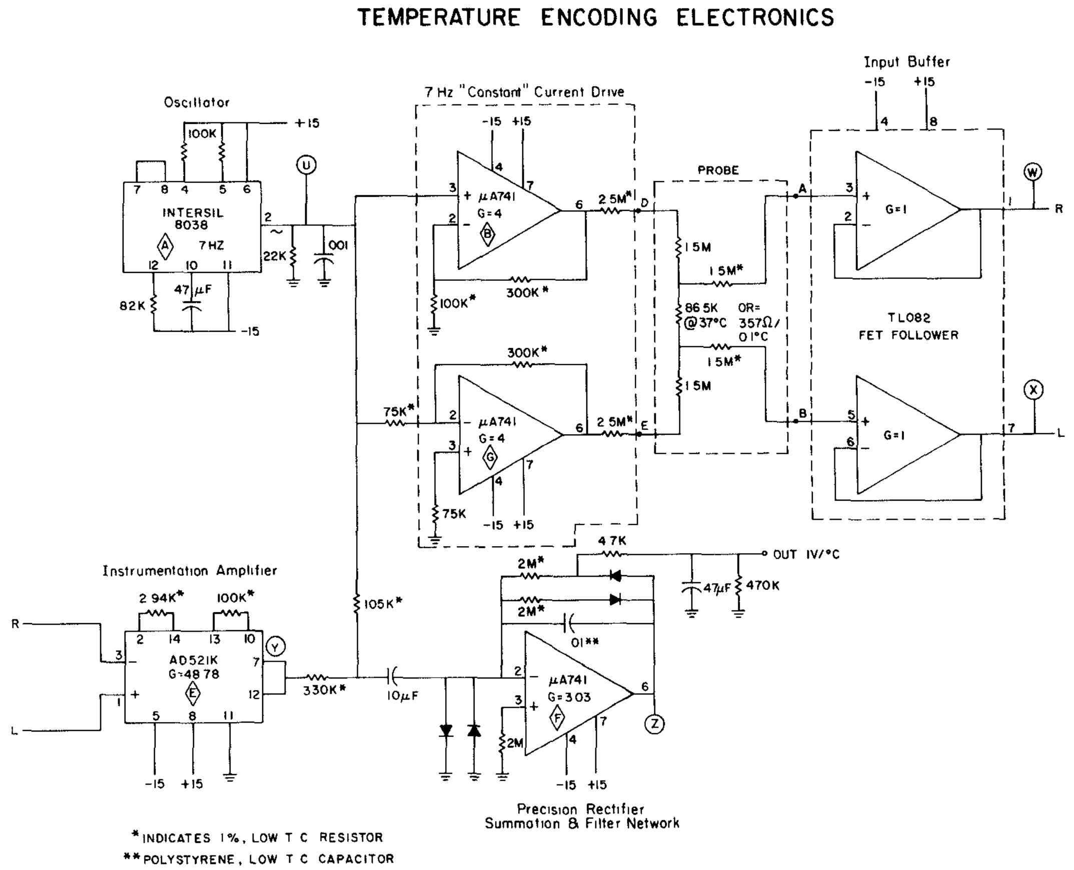

Fig. 2. A schematic diagram of the temperature encoding electronics, exclusive of the power supply.

necessary in order to reduce thermal diffusion. The methods for field-perturbation testing were essentially the same before and after design as used previously [1]. That is, a 3-cm radius sphere of brain tissue phantom was exposed to far field 2450 MHz at a predetermined power density and exposure duration after which thermographic scans mapped the thermal analog of the induced field distribution. The electrode was then inserted, either after cooling of the original target or in another identical target, and the exposure regime was repeated with thermographic scans. To the extent that the electrode affected field induction in the brain phantom, the two heating patterns would be different.

Thermographic testing of the thin-film line took place in air. Short segments (2 in) were used with thermographic line scans at the center of the line segment. This arrangement obviated the need for two-dimensional scans to find the location of peaks in the current distribution (a very difficult procedure for quantitative testing due to the rapid dissipation of heat which gave erroneously low values because of the 4-s frame time for high resolution two-dimensional imagery). The short segments could be analyzed by a single-line scan in the geometric center of the line segment. Under these conditions, the line segment was a short dipole in which a triangular current distribution would produce peak heating in the geometric center. Standing waves would be detectable in the two-dimensional scans in the phantom, since all of these scans were for complete electrodes including the connector and shell.

Thermographic testing of the complete electrode took place in the brain phantom. The electrodes were located in the brain phantom at a distance of 10 mm from the leading edge of the sphere, and at a depth such that the 200-kΩ thick-film segment operated in air with 5 mm of exposed length beyond the brain. Thin-film line, of course, operated totally in air.

Thermometric evaluation of the electrodes required the development of a temperature encoding electronic package shown schematically in Fig. 2. The circuit consisted of an IC constant current generator operating at 7 Hz to drive the thermistor with 100 μA over one unshorted pair of lines. The voltage detector consisted of two high-input impedance (10^9-Ω) buffers followed by an IC instrumentation amperage with high common mode rejection ratio (90 dB) and frequency shaped gain via the feedback network. The lines for voltage detection were, of course, the remaining unshorted pair of lines. Output voltage was measured by an HP 3440A digital voltmeter. Chart records were made on an HP 7100B after processing by an HP 580A digital-to-analog converter. The system was tested in a Leeds & Northrup 8401 oil bath with better than millidegree regulation. Bath temperature was

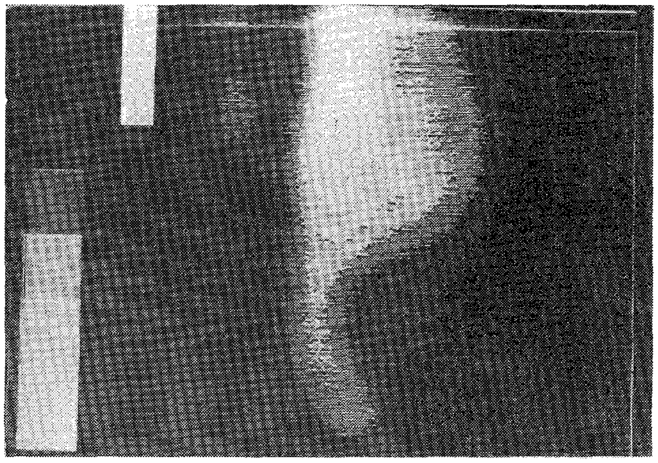

Fig. 3. A thermograph of a four-terminal design with four PTFE lines. The four-terminal point is at the upper substrate section. All grey scale thermographs are block quanitized with a 3-°C range and isometrically displayed.

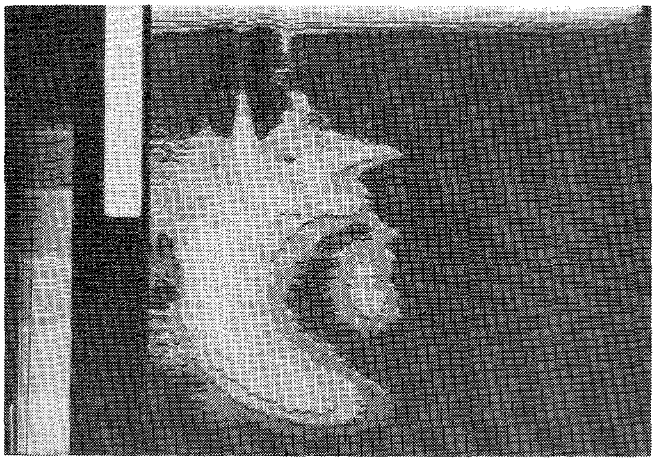

Fig. 4. A thermograph of a four-terminal design with four hyperthin lines and four nontapered thick-film lines to the sensor. The short vertical heat source at left center is that portion of the thick-film line which extends beyond the brain phantom.

monitored with an HP 2801A quartz thermometer. The electrode was first tested for stability over a four-day period. After this, the bath was slewed over a temperature range of 35–40°C, and back to 35°C over an eight-hour period for RT calibration and hysteresis testing. This procedure was repeated four times over a seven-day period.

III. Results

Thermographic evaluation of the electrode revealed that thermal analogs of field aberrations could be either in the direction of heat sourcing or in the direction of heat sinking. An inadequately decoupled electrode may serve as a heat source. Fig. 3 illustrates heating due to the PTFE line which diffuses down the substrate into the brain phantom. When the PTFE line is replaced with the hyperthin line, only the upper thick-film section which operates in air contributes a heat-source artifact as shown in Fig. 4.

The vastly different loss of air and brain and/or standing waves at the air–dielectric interface produced the heating observed at the upper portion of the transducer subassembly, where it extends beyond the border of the brain phantom as shown in Fig. 4. Note the absence of heating in the four hyperthin lines. The conflicting requirements of operation in both air and brain for the transducer subassembly could be reconciled by linearly tapering the thick-film electrode, from the highest value of resistance at the proximal end of the substrate which operates in air to the lowest value of resistance at the distal end which is embedded in brain. The result with this configuration is shown in Fig. 5. Only a slight heat sinking is detectable in the before and after line scans taken at the location of the electrode tip in the brain phantom, and no heat sourcing is evident as shown in Fig. 6(a) and (b).

Line scans through the 10-mil-wide hyperthin film conductors (200 kΩ/in) in air are shown in Fig. 7. There is virtually no detectable heating in the line. Lower resistance hyperthin line (25 kΩ/in) maybe compared to PTFE line of the same lineal resistance and width. Width matching is necessary in order that the effects of the modulation transfer function (MTF) of the infrared imaging system are constant. The resolution of the IR scan is 2 mrad. This means that the MTF is 3 dB down at a 16-in working distance for two ideal IR point sources 16 mil apart. The hyperthin line and the PTFE line are shown in Fig. 8(a) and (b), respectively. Approximately 1°C heating is evident in both, but the hyperthin lines appears to heat slightly less. The standing waves were detected with wide PTFE lines (i.e., about 100 mil) as seen in Fig. 9. These could not be detected with the hyperthin line.

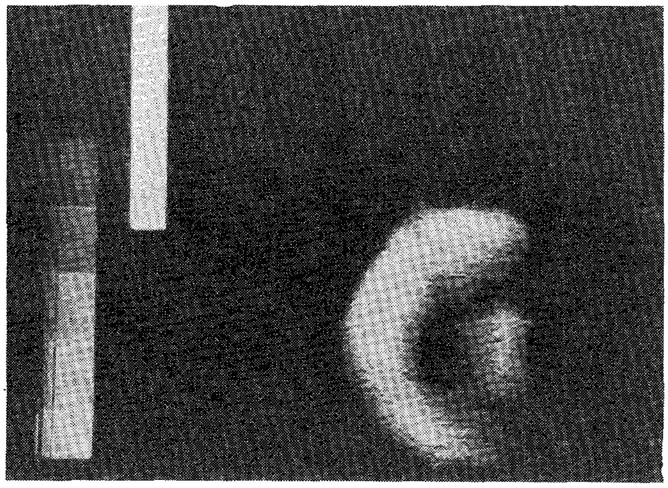

Fig. 5. A thermograph of a four-terminal design of construction similar to that in Fig. 4, except that the thick-film line is tapered in width to increase its lineal resistance from 50 kΩ/in at the distal end to 200 kΩ/in at the proximal end.

Thermometric evaluation with the temperature encoding electronics in room air, and the transducer in a regulated oil bath disclosed environmental temperature sensitivity in the temperature encoding electronics, such that a 1°C change in room temperature produced a 20 millidegree apparent change in the measurand of the opposite

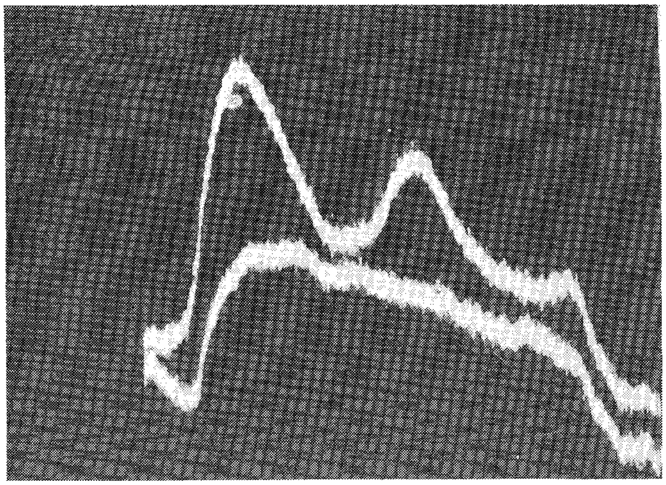

(a)

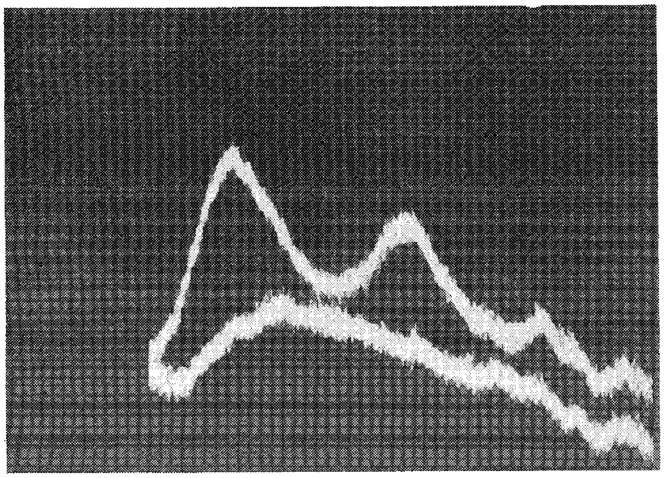

(b)

Fig. 6. (a) A line scan pair with full-scale temperature of 3°C taken at the location in the brain phantom where the electrode tip will be in (b). The upper scan line demonstrates heating in the brain phantom in the absence of the electrode, while the lower scan line represents thermal gradients in the phantom prior to microwave exposure. (b) A line scan pair taken under the same conditions as (a) except that the four-terminal MIC temperature electrode is in place. Note that the increment in the first peak is lower than that in (a) as a result of slight heat sinking due to the electrode.

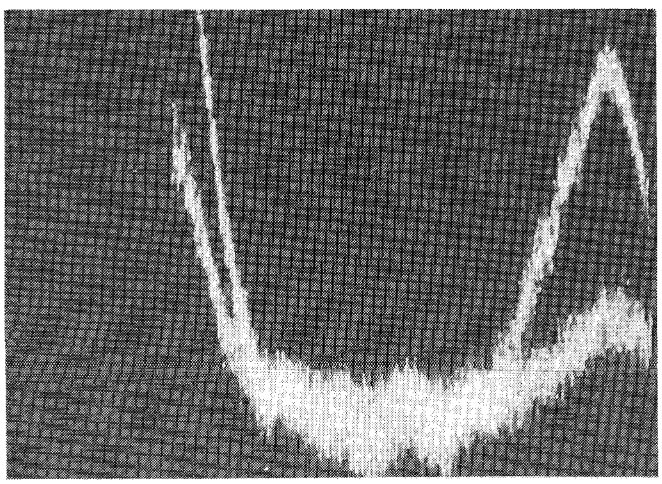

Fig. 7. A line scan pair taken in air at the center of a 2-in hyperthin line (200 kΩ/in) segment. Note that heating in the line is within the noise equivalent temperature of the thermograph.

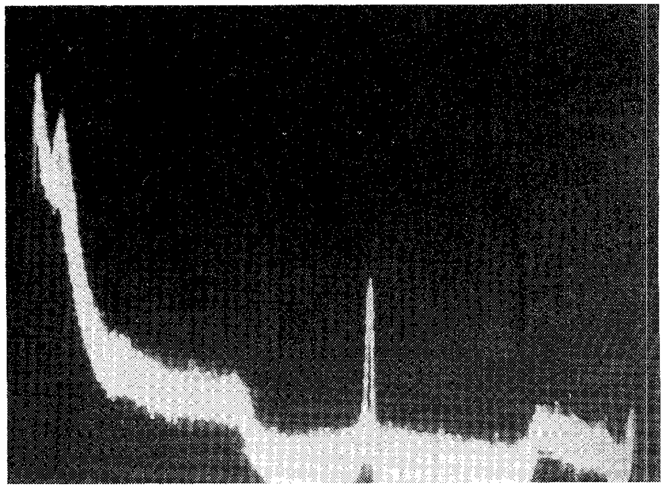

(a)

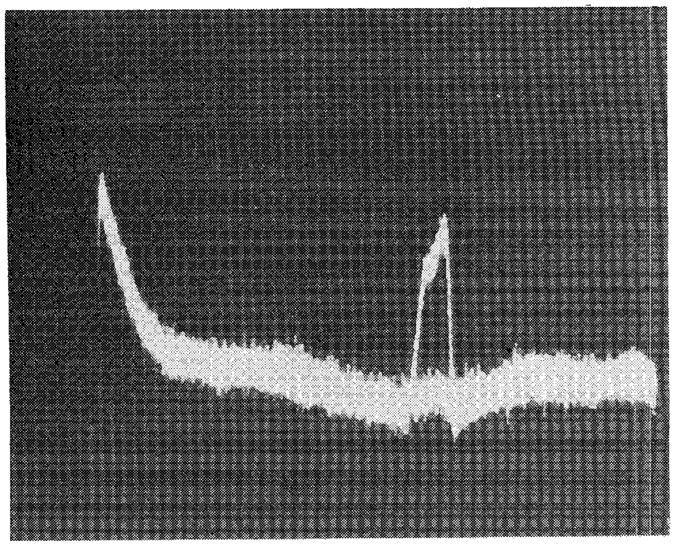

(b)

Fig. 8. (a) A line scan pair taken in air at the center of a 2-in section of PTFE line (50 kΩ/in). (b) A line scan pair taken in air at the center of a 2-in hyperthin line (50 kΩ/cm) contained in Tygon tubing. Note that the height of the heating peaks in the line scans are comparable. The greater width of the peak represents the tubing cover.

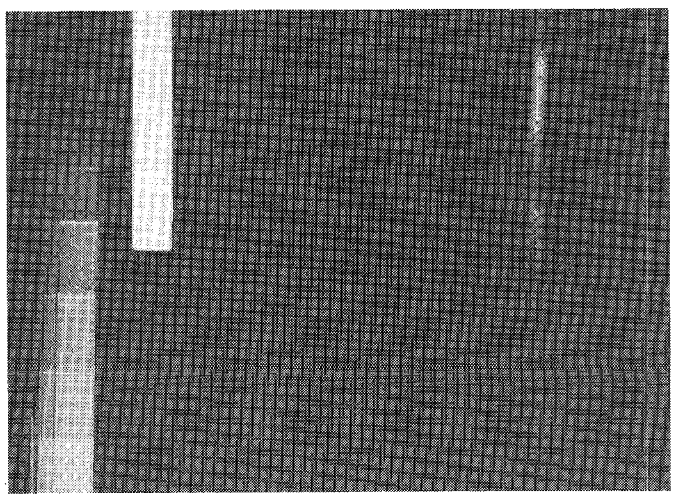

Fig. 9. A thermograph of wide PTFE line which suggests standing waves. The mode spacing is about 1.2 cm.

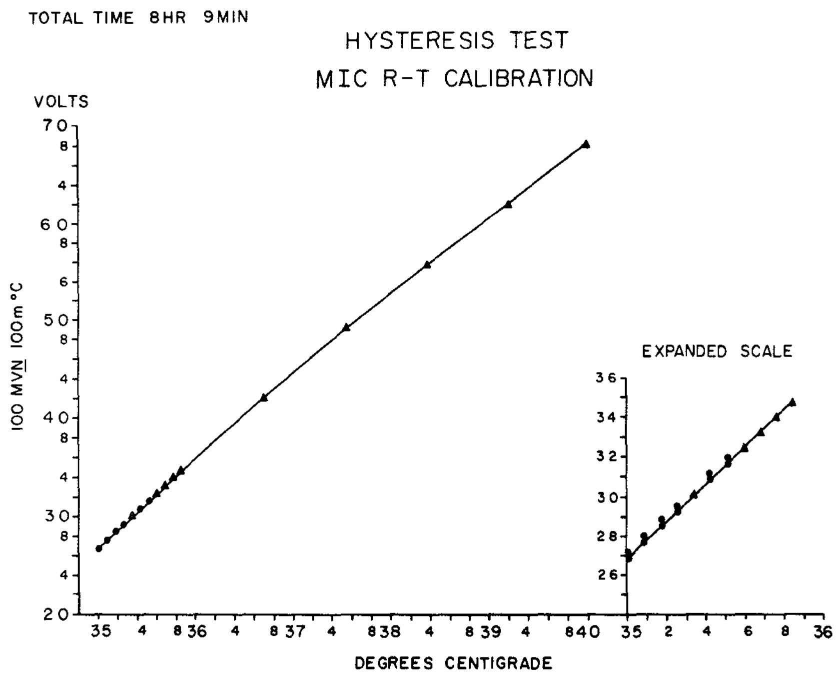

Fig. 10. A hysteresis test of the completed electrode and temperature encoding electronics. The data represent an 8-h run with bath temperature slewed from 35°C to 40°C, and back to 35°C.

direction. Stability tests in temperature controlled conditions established the resolution of the system to be determined by a noise equivalent temperature of about 7 millidegrees. Long term stability proved to be largely determined by variations in room temperature. Over a single 8-h hyteresis test, the ascending and descending $V-T$ curves were largely superimposed except for a 10 millidegree discrepancy at the end of the run as shown in Fig. 10. On two successive days, the $V-T$ curves tracked within 25 millidegrees. On replications over five days, the $V-T$ curves tracked within the design goal of 100 millidegrees.

IV. Discussion

The concept of electrothermal matching has important implications for the limits of performance that can be expected from thermometric system which must operate in tissue during microwave exposure. The ideal situation would be an electrode which matched its loss to the equivalent volume of tissue it displaces. Unfortunately, this is not possible due to the fact that the loss tangent of tissue is not static. Rather, the microwave properties of tissue is constantly changing due to such things as regional blood flow, and physiological responses to incident radiation. This implies that it is not possible to match losses except at some arbitrary condition. Similarly, it follows that different electrodes must be used for different tissue, at least to the extent that very low water content tissue such as bone will require a different electrode than very high water content tissue such as aqueous humor of the eye. Indeed the direction of the artifact may be predicted: the brain electrode will heat sink aqueous humor and heat source bone. Obviously, an electrode which must operate in air has still different requirements. If the present electrode was to operate in air, e.g., at the surface of the skin, the best procedure would be to place the sensor at the end of the thin-film transmission lines, without the tissue specific matching in the thick-film segment.

The hyperthin line proved to be quite robust once the fabrication error due to thermal cycling was discovered. It can sustain handling and bending without fracture so long as crimping is avoided. A comparison of the hyperthin and PTFE lines emphasizes the ease and stability of connection to the hyperthin line at high-lineal resistances, about 200 kΩ/in. The former's slightly lower heating may represent the relatively higher ac resistance of the hyperthin line possibly due to its 30-Å conductor depth in comparison to the PTFE which is many skin depths thick. Emissivity differences do confound the comparison, however.

The thermal conductivity of the electrode is another matter of importance if it must traverse regions where temperature gradients exist. As was pointed out by Larsen *et al.* [1], there is a 0.5°C gradient between cortex and brain stem due to circulatory patterns. It is important that the electrode have the lowest thermal conductivity and the best loss match possible. The thermal conductivity of the hyperthin line is extremely low due its aspect ratio. The thick-film substrate chosen was porcelain with an air-filled center in order to minimize thermal conductivity. This design also minimized thermal mass to improve the thermal time constant. Preliminary observations indicate a thermal time constant value of approximately 10 ms.

The transmission line is an especially important issue in four-terminal designs since the heating is additive. Also coupling between lines appears to decrease its ac resistance.

The temperature encoding electronics also represent a design problem. It is notable that the present design offers much lower common mode voltages by floating the current source. Circuit testing with local freezing indicates that maximum temperature coefficient effects reside in the instrumentation amplifier. The use of a dual IC with FET inputs for the buffer stage also offers better temperature coefficient than two separate buffers with bipolar inputs. AC drive at low frequency was selected in order to alleviate phase differences that could simulate differential voltages. DC drive was rejected due to detection problems.

Future directions will include development of a monolithic version of the temperature-encoding electronics with improved environmental stability. The package will also include provision for telemetry with suitable resistance to RFI in order to operate in microwave environments. We have begun work also on a totally flexible electrode for use where stereotaxic implantation is either unnecessary or undesirable (e.g., intravascular or intraluminal use).

V. Conclusion

Temperature measurement in biological dielectrics does profit from the concept of electrothermal matching, whereby artifact introduced by the thermometer maybe in either of two directions: heat sinking or heat sourcing. Insofar as the complex permittivity of biological dielectrics is physiologically variable, there is an upper limit to which this artifact maybe reduced. The electrode, herein described, is relatively free from heat sinking or heat sourcing for 250-mW/cm^2 2450-MHz fields within phantom brain and air environments for the transducer subassembly and flexible hyperthin line, respectively. At the electrode tip, heat sinking is in the order of 0.15°C. Further development will require total system operation in microwave environment with freedom from RFI and temperature coefficient effects in the temperature encoding and telemetry electronics.

References

[1] L. E. Larsen, R. A. Moore, and J. Acevedo, "A microwave decoupled brain-temperature transducer," *IEEE Trans. Microwave Theory and Tech.*, vol. MTT-22, pp. 438–444, 1974.

[2] C. C. Johnson and A. W. Guy, "Nonionizing electromagnetic wave effects in biological materials and systems," *Proc. IEEE*, vol. 60, pp. 692–719, 1972.

[3] R. R. Bowman, "Fabricating high resistance transmission lines," in *NBS Memo. Rec.*, 1970.

[4] T. C. Cetas, "Temperature measurement in microwave diathermy fields: Principles and probes," *Proc. Int. Symp. Cancer Therapy by Hyperthermia and Radiation*, J. E. Robinson Ed., Am. Col. Radiology, Bethesda, p. 193, 1976.

[5] F. B. Silsbee, "Notes on the design of four terminal resistance standards for alternating current," NBS Research Paper #133, 1930.

[6] S. B. Cohn, "Slot line—An alternative transmission medium for integrated circuits," in *IEEE G-MTT Int'l. Symp. Dig.*, p. 104–109, 1968.

The Modal Spectrum of a Lossy Ferrimagnetic Slab

FERNANDO BARDATI, MEMBER, IEEE, AND PAOLO LAMPARIELLO, MEMBER IEEE

***Abstract*—The propagation of electromagnetic waves on a lossy ferrimagnetic slab is considered. Direction of propagation, dc external magnetic field, and surface normals are assumed at right angles. Modal curves, assuming the width of the slab and the frequency as parameters, are presented. In general, the modes corresponding to propagating as well as attenuating waves are confined to the vicinity of the slab in a frequency range greater than is the case for no magnetic losses. Magnetostatic and half-space approximations are discussed.**

Manuscript received August 8, 1977; revised August 7, 1978. This work was supported in part by the Consiglio Nazionale delle Ricerche of Italy.

The authors are with the Istituto di Elettronica, University of Rome, Rome, Italy.

I. Introduction

THE interest in theoretical and experimental analysis of electromagnetic waves supported by layered structures containing ferrimagnetic-dielectric materials has grown in the last few years together with the progress in the technology of microwave-microstrip components. The ferrite-dielectric and ferrite-metal discontinuities, already discussed by authors who have dealt with the electromagnetic propagation in waveguides loaded with ferrite (for a comprehensive treatment, see [1]), have recently received renewed attention [2]–[6]; the main purpose being to establish the existence of surface waves guided by such discontinuities. The wave propagation on

0018-9480/79/0700-0679$00.75 ©1979 IEEE